

PAPER • OPEN ACCESS

Linear response of zero-resistance states

To cite this article: Maxim Breitzkreiz 2017 *New J. Phys.* **19** 083006

View the [article online](#) for updates and enhancements.

Related content

- [The correlation between the Nernst effect and fluctuation diamagnetism in strongly fluctuating superconductors](#)
Kingshuk Sarkar, Sumilan Banerjee, Subroto Mukerjee et al.
- [Evanescent-wave Johnson noise in small devices](#)
Vickram N Premakumar, Maxim G Vavilov and Robert Joynt
- [Symmetries in Hall-like systems: microwave and nonlinear transport effects](#)
Manuel Torres and Alejandro Kunold



PAPER

Linear response of zero-resistance states

OPEN ACCESS

RECEIVED
12 April 2017REVISED
13 June 2017ACCEPTED FOR PUBLICATION
4 July 2017PUBLISHED
8 August 2017Original content from this
work may be used under
the terms of the [Creative
Commons Attribution 3.0
licence](https://creativecommons.org/licenses/by/4.0/).Any further distribution of
this work must maintain
attribution to the
author(s) and the title of
the work, journal citation
and DOI.

Maxim Breitzkreiz

Instituut-Lorentz, Universiteit Leiden, PO Box 9506, 2300 RA Leiden, Netherlands

E-mail: breitzkreiz@lorentz.leidenuniv.nl

Keywords: zero-resistance states, MIRO, 2D electron gas

Abstract

A two-dimensional electron system in the presence of a magnetic field and microwave irradiation can undergo a phase transition towards a zero-resistance state (ZRS). A widely used model predicts the ZRS to be a domain state, which responds to applied dc voltages or dc currents by slightly changing the domain structure. Here we propose an alternative response scenario, according to which the domain pattern remains unchanged. Surprisingly, a fixed domain pattern does not destroy zero-resistance, provided that the resistance is direction independent. Otherwise, if the symmetry of the domain pattern allows a direction dependence of the resistance, the domain state can be dissipative. We give examples for both situations and simulate the response behavior numerically.

1. Introduction

At the beginning of this century, Mani *et al* [1] and Zudov *et al* [2] discovered a new dissipationless state of a 2D electron gas that is exposed to microwave irradiation and an out-of-plane magnetic field [3]. Upon entering this so-called zero-resistance state (ZRS), the longitudinal conductivity of the sample drops to zero, while the Hall conductivity, unlike in the quantum Hall effect, does not show any discontinuity. Great experimental and theoretical efforts have been made to understand this phenomenon, yielding at present strikingly different explanations. While theories involving pondermotive forces near the contacts [4] or the effect of radiation on edge states [5] seem to be less likely in view of recent measurements [6], other theories, predicting the ZRS to be either homogeneous or inhomogeneous, constitute competing alternatives. The radiation-driven electron orbit model combines semiclassics with an exact solution of a quantum-harmonic-oscillator problem and explains the ZRS in terms wave-packet dynamics and Pauli exclusion principle [7]. According to this theory the ZRS is homogeneous.

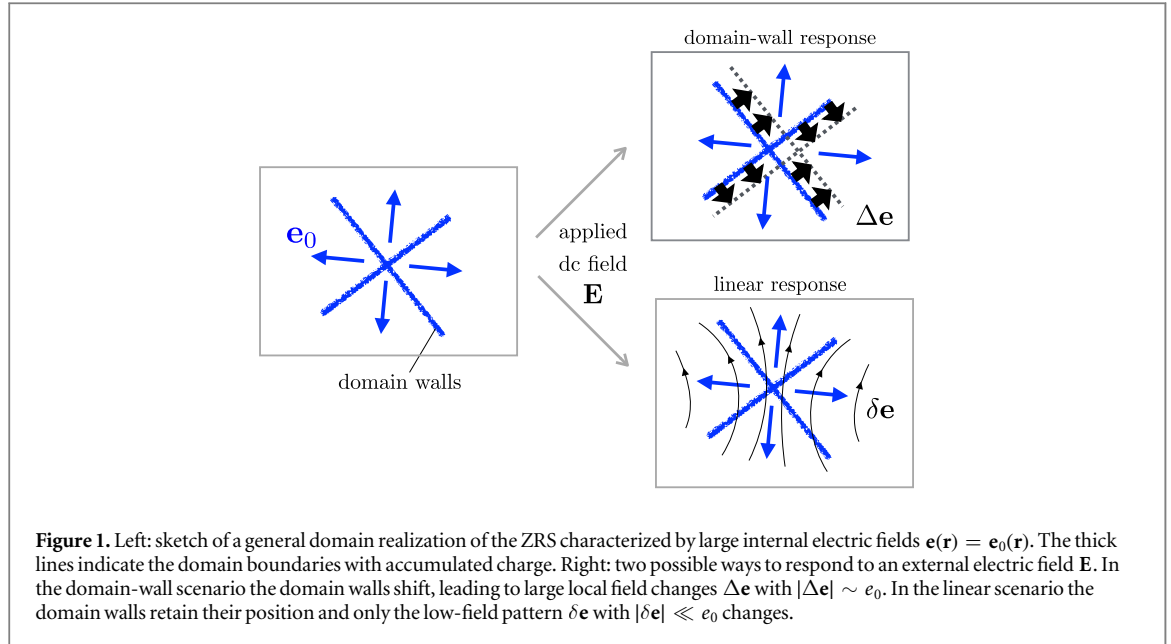
An in turn different group of theoretical models instead predicts that the ZRS is an inhomogeneous domain state. Here the basic mechanism can be understood via a combination of microscopic calculations of the non-equilibrium state [8–11] and considerations of the electrodynamics of the system [12–15].

This work is based on the domain-state model, which we will now introduce in more detail. Microscopic calculations show that the interplay of photon absorption and scattering of the electrons lead to a longitudinal conductivity that oscillates upon changing the microwave frequency, the magnetic field strength, or the electric field strength. For fixed frequency and magnetic field, the conductivity tensor, i.e., the tensor that relates the local electric field $\mathbf{e}(\mathbf{r})$ and the local current density, $\mathbf{j}(\mathbf{r}) = \sigma(e)\mathbf{e}(\mathbf{r})$, can be approximated as [16]

$$\sigma(e) = \begin{pmatrix} \sigma_d(e) & \sigma_H \\ -\sigma_H & \sigma_d(e) \end{pmatrix}, \quad (1)$$

where the dissipative part σ_d depends on the absolute value of the local electric field, $e \equiv |\mathbf{e}(\mathbf{r})|$. In the parameter range of the ZRS, the dissipative part is negative at $e = 0$ and becomes positive only above a critical value e_0 , with $\sigma'_d(e_0) \equiv d\sigma_d(e_0)/de > 0$. This critical field strength is set by the radiation field and is thus typically much larger than an external dc field of a linear-response measurement [9].

Naively the theoretical prediction of negative $\sigma_d(0)$ seems to imply a negative-resistance state instead of a ZRS. This however is only true if the system is assumed to be homogeneous and the effect of boundaries and contacts can be neglected. Indeed, numerical simulations of a system with boundaries, fixed homogeneous



charge distribution, and negative $\sigma_d(0)$ predict the resistance to have positive dissipative part and a sign-reversed Hall part [17], which, however, still contradicts experimental observations.

A different ansatz is to allow for an inhomogeneous charge distribution. In this case, neglecting boundary and contact effects, a conventional linear-response experiment measures the *effective conductivity* Σ , which determines the linear relation

$$\mathbf{J} = \Sigma \mathbf{E} \quad (2)$$

between the spatially averaged electric field $\mathbf{E} = \langle \mathbf{e}(\mathbf{r}) \rangle$ and current density $\mathbf{J} = \langle \mathbf{j}(\mathbf{r}) \rangle$, where $\langle \dots \rangle \equiv \int d^2r \dots / V$ denotes the spatial average over the sample volume V . Generally, in inhomogeneous systems the local conductivity σ does not coincide with the effective conductivity Σ . Inhomogeneities in turn can be stabilized if the local conductivity is not positive semidefinite [18], which is the case in the regime of the ZRS for $e < e_0$. Andreev *et al* [12] thus proposed that upon entering the ZRS, the system undergoes a dynamical phase transition towards a state with an inhomogeneous internal electric space field

$$\mathbf{e}(\mathbf{r}) = \mathbf{e}_0(\mathbf{r}), \quad (3)$$

which direction can vary in space but the magnitude is fixed to e_0 everywhere, barring isolated singular points and lines. For the average field to vanish, the system must form domains [12, 13, 15, 16] with accumulated charge at domain boundaries, as sketched in figure 1. It has been shown that time-dependent fluctuations around $\mathbf{e}_0(\mathbf{r})$ do not diverge with time, signifying the stability of a steady domain state characterized by (3) [12, 13].

The restriction (3) allows for a variety of possible field patterns $\mathbf{e}_0(\mathbf{r})$ that can be formed upon entering the ZRS regime. While in clean systems the system tends to minimize the total length of domain boundaries, impurities can make the domain pattern more complex and disordered [13, 14]. Measurements that are sensitive to local field changes provide experimental support for the domain-state model [19, 20] and indicate that the pattern tends to be rather complex [21]. An unambiguous evidence for the existence of domains, however, is still missing and the exact shape and size, could not be observed so far.

In the following we assume that the system is in a domain state with an arbitrary domain pattern and focus on the response of the domain state to an external homogeneous dc electric field \mathbf{E} or an imposed current density \mathbf{J} . Assuming that each domain state must strictly satisfy (3), one can obtain the effective conductivity by averaging the microscopic relation $\mathbf{j}(\mathbf{r}) = \sigma(e_0)\mathbf{e}_0(\mathbf{r})$ and comparing with (2), giving

$$\Sigma = \sigma(e_0) = \begin{pmatrix} 0 & \sigma_H \\ -\sigma_H & 0 \end{pmatrix}, \quad (4)$$

which is in agreement with experiments. The interpretation of the response mechanism is then the following: switching on an infinitesimal electric field \mathbf{E} , the system responds in form of an infinitesimal shift of the domain walls, as sketched in figure 1. Compared to the initial state $\mathbf{e}_0(\mathbf{r})$, some domains become shrunk, other domains become expanded such that the final state $\tilde{\mathbf{e}}_0(\mathbf{r}) = \mathbf{e}_0(\mathbf{r}) + \Delta \mathbf{e}(\mathbf{r})$ satisfies the new boundary condition, $\langle \tilde{\mathbf{e}}_0(\mathbf{r}) \rangle = \mathbf{E}$. The induced field changes $\Delta \mathbf{e}(\mathbf{r})$ are zero everywhere except at domain boundaries, where they are huge ($\sim e_0$), thus constituting a locally *nonlinear* response.

In this work, we argue that the response of the domain state can be locally linear and must not involve domain-wall shifting. Our scenario, which we will call *linear scenario*, involves only small changes of the local electric field $\delta\mathbf{e}(\mathbf{r})$, as sketched in figure 1. In general, this microscopically different mechanism results in a different effective conductivity, the determination of which turns out to be more difficult than in the domain-wall scenario. We will derive general symmetry relations that restrict the space of possible effective-conductivity tensors. These relations fix the effective conductivity to (4) only if the effective conductivity is isotropic. In the anisotropic case we instead find that the domain state can be dissipative.

The outline of this work is as follows. First we define the linear-response scenario. In section 3 we consider the effective conductivity in this scenario, and separately discuss the isotropic and the anisotropic cases. In section 4 we discuss the time relaxation of the ZRS that is brought out of the steady state by a dc voltage for two examples. We conclude in section 5.

2. Linear-response states

We define a linear-response state as $\mathbf{e}(\mathbf{r}) = \mathbf{e}_0(\mathbf{r}) + \delta\mathbf{e}(\mathbf{r})$, composed of a high-field pattern $\mathbf{e}_0(\mathbf{r})$ with $|\mathbf{e}_0(\mathbf{r})| = e_0$ [12], that averages to zero, and a low-field pattern $\delta\mathbf{e}(\mathbf{r})$ with $|\delta\mathbf{e}(\mathbf{r})| \ll e_0$ that averages to the external electric field to meet the imposed boundary condition $\langle \mathbf{e}(\mathbf{r}) \rangle = \mathbf{E}$.

The steady high-field pattern $\mathbf{e}_0(\mathbf{r})$ is rotation free and the corresponding current density $\mathbf{j}_0(\mathbf{r}) = \sigma(e_0)\mathbf{e}_0(\mathbf{r})$ satisfies the stationary continuity equation. Mathematically, it is thus the solution of the differential equations

$$\nabla \cdot \mathbf{j}_0(\mathbf{r}) = 0, \quad \nabla \times \mathbf{e}_0(\mathbf{r}) = 0, \quad (5)$$

with the boundary condition $\langle \mathbf{e}_0(\mathbf{r}) \rangle = 0$.

Similarly, a steady linear-response state with the current density $\mathbf{j}(\mathbf{r}) = \sigma(e)\mathbf{e}(\mathbf{r})$ and the electric field pattern $\mathbf{e}(\mathbf{r})$ must solve the same differential equation (5) with the boundary condition $\langle \mathbf{e}(\mathbf{r}) \rangle = \mathbf{E}$. Due to linearity of the differential operators in equation (5) and the spatial average $\langle \dots \rangle$, this is equivalent to the requirement of a steady low-field subsystem $\delta\mathbf{e}(\mathbf{r})$, $\delta\mathbf{j}(\mathbf{r})$, which then is the solution of

$$\nabla \cdot \delta\mathbf{j}(\mathbf{r}) = 0, \quad \nabla \times \delta\mathbf{e}(\mathbf{r}) = 0, \quad (6)$$

with the boundary condition $\langle \delta\mathbf{e}(\mathbf{r}) \rangle = \mathbf{E}$. The current density of the low-field system is obtained by subtracting $\mathbf{j}_0(\mathbf{r}) = \sigma(e_0)\mathbf{e}_0(\mathbf{r})$ from $\mathbf{j}(\mathbf{r}) = \sigma(e)\mathbf{e}(\mathbf{r})$ and expanding to linear order in $\delta\mathbf{e}(\mathbf{r})$ giving

$$\delta\mathbf{j}(\mathbf{r}) = \tilde{\sigma}(\mathbf{r})\delta\mathbf{e}(\mathbf{r}), \quad (7)$$

with the local conductivity

$$\begin{aligned} \tilde{\sigma}(\mathbf{r}) &= \sigma(e_0) + \sigma_D \hat{\mathbf{e}}_0(\mathbf{r}) \otimes \hat{\mathbf{e}}_0(\mathbf{r}) \\ &= \begin{pmatrix} 0 & \sigma_H \\ -\sigma_H & 0 \end{pmatrix} \\ &+ \sigma_D \begin{pmatrix} \cos^2 \phi(\mathbf{r}) & \cos \phi(\mathbf{r}) \sin \phi(\mathbf{r}) \\ \cos \phi(\mathbf{r}) \sin \phi(\mathbf{r}) & \sin^2 \phi(\mathbf{r}) \end{pmatrix}, \end{aligned} \quad (8)$$

where $\sigma_D \equiv \sigma'_d(e_0)e_0$ and $\hat{\mathbf{e}}_0(\mathbf{r}) = \mathbf{e}_0(\mathbf{r})/e_0 = (\cos \phi(\mathbf{r}), \sin \phi(\mathbf{r}))$ is the direction of the high-field electric field, parametrized by the polar angle $\phi(\mathbf{r})$.

The key observation is that the electrodynamics of the low-field subsystem resembles the electrodynamics of a conventional inhomogeneous conductor [22], with an \mathbf{r} -dependent conductivity $\tilde{\sigma}(\mathbf{r})$, a local electric field $\delta\mathbf{e}(\mathbf{r})$, and a local current density $\delta\mathbf{j}(\mathbf{r})$ that are induced by the external electric field \mathbf{E} . Like for a conventional conductor, the stability of the steady low-field subsystem is thus guaranteed by the positive semidefiniteness of the symmetric part of the local conductivity $\tilde{\sigma}(\mathbf{r})$. From (9), this is easily proven to be satisfied for any high-field pattern $\mathbf{e}_0(\mathbf{r})$ for all \mathbf{r} . A more explicit discussion of the stability is presented in section 4.

3. Effective conductivity

Given that the domain state responds according to the linear scenario instead of moving the domain walls, we now consider its effective conductivity. Particularly interesting is the question whether the domain state is a ZRS if the system responds according to the linear scenario, i.e., the field pattern slightly deviates from a pure domain state $\mathbf{e}_0(\mathbf{r})$.

For a given $\tilde{\sigma}(\mathbf{r})$ the effective conductivity Σ can be defined as

$$\Sigma \langle \delta\mathbf{e}(\mathbf{r}) \rangle = \langle \tilde{\sigma}(\mathbf{r})\delta\mathbf{e}(\mathbf{r}) \rangle \quad (10)$$

for all possible $\delta\mathbf{e}(\mathbf{r})$. From this definition it is in general difficult to calculate Σ explicitly. However, thanks to a certain symmetry inherent in the electrodynamics of 2D systems, which has been found by Dykhne in 1971 [23], we can derive exact symmetry relations that restrict the space of possible tensors Σ .

We introduce new fields $\delta\mathbf{j}'(\mathbf{r})$ and $\delta\mathbf{e}'(\mathbf{r})$ via the transformation

$$\delta\mathbf{j}(\mathbf{r}) = \delta\mathbf{j}'(\mathbf{r}) + \sigma_H R \delta\mathbf{e}'(\mathbf{r}), \quad (11)$$

$$\delta\mathbf{e}(\mathbf{r}) = 3 \delta\mathbf{e}'(\mathbf{r}) + \sigma_H^{-1} R \delta\mathbf{j}'(\mathbf{r}), \quad (12)$$

where R is a 90° -rotation matrix. Using the 2D-specific relations

$$\nabla \cdot R \mathbf{v} = -\nabla \times \mathbf{v} \quad \text{and} \quad \nabla \times R \mathbf{v} = \nabla \cdot \mathbf{v}, \quad (13)$$

one can easily show that the new fields are another solution of (6) and (7) with the same conductivity tensor (9), like the original fields. The two solutions correspond to different boundary conditions, i.e., the averaged fields $\mathbf{J}' = \langle \delta\mathbf{j}'(\mathbf{r}) \rangle$ and $\mathbf{E}' = \langle \delta\mathbf{e}'(\mathbf{r}) \rangle$ differ, in general, from \mathbf{J} and \mathbf{E} . The effective conductivity, however, does not depend on the fields, so \mathbf{J}' and \mathbf{E}' must be related by the same effective conductivity Σ as the fields \mathbf{J} and \mathbf{E} . Averaging equations (11) and (12), and using $\mathbf{J}' = \Sigma \mathbf{E}'$ and $\mathbf{J} = \Sigma \mathbf{E}$, we find

$$\Sigma = (1 - \sigma_H^{-1} \Sigma R)^{-1} (3 \Sigma - \sigma_H R). \quad (14)$$

For a general effective conductivity tensor, this relation is equivalent to

$$\det \Sigma = \sigma_H^2, \quad (15)$$

$$\Sigma_{12} - \Sigma_{21} = 2 \sigma_H, \quad (16)$$

where Σ_{ij} are the components of Σ . Note that equations (15) and (16) hold for an arbitrary domain pattern. It can be easily seen that a conductivity tensor satisfying (15) and (16) is positive semidefinite, which allows for dissipationless as well as dissipative response.

3.1. Isotropic effective conductivity

Isotropy, i.e., direction independence of the effective conductivity imposes two additional equations,

$$\Sigma_{11} = \Sigma_{22}, \quad \Sigma_{12} = -\Sigma_{21}. \quad (17)$$

Together with the derived symmetry relations (15) and (16) this fixes the effective conductivity unambiguously to

$$\Sigma = \begin{pmatrix} 0 & \sigma_H \\ -\sigma_H & 0 \end{pmatrix}. \quad (18)$$

This shows that a domain state with an isotropic effective conductivity is indeed a ZRS. The linear scenario thus correctly reproduces the experiments [1, 2] in this case. Isotropy of the effective conductivity can be assumed if the domain pattern has four-fold rotational (C_4) symmetry, or the domain pattern is randomized by impurities [13, 14].

3.2. Anisotropic effective conductivity

Without additional restrictions on the effective conductivity, equations (15) and (16) no longer guarantee the absence of dissipation. In fact, the response can be dissipative in this case, which we show now by calculating the effective conductivity for a specific domain pattern.

We consider a model with a single domain wall separating two domains with opposite directions of \mathbf{e}_0 , as illustrated in figure 2(a). Inserting these directions into equation (9) we find

$$\tilde{\sigma}(\mathbf{r}) = \begin{pmatrix} 0 & \sigma_H \\ -\sigma_H & \sigma_D \end{pmatrix}. \quad (19)$$

For this simple structure the local conductivity (9) is the same in both domains and thus, according to (10), equal to the effective conductivity,

$$\Sigma = \begin{pmatrix} 0 & \sigma_H \\ -\sigma_H & \sigma_D \end{pmatrix}. \quad (20)$$

Since $\sigma_D > 0$ the response is dissipative in contrast to the prediction of the domain-wall scenario [12].

4. Dynamical response

So far we have discussed the possibility of the linear scenario as an alternative to the domain-wall scenario in the steady regime, i.e., at times when the system had enough time to rearrange the charge density $\delta n(\mathbf{r}, t)$ after the application of an external field \mathbf{E} . To decide, which type of response the system will choose, we now consider the time dependence of the charge density right after the application of an external field.

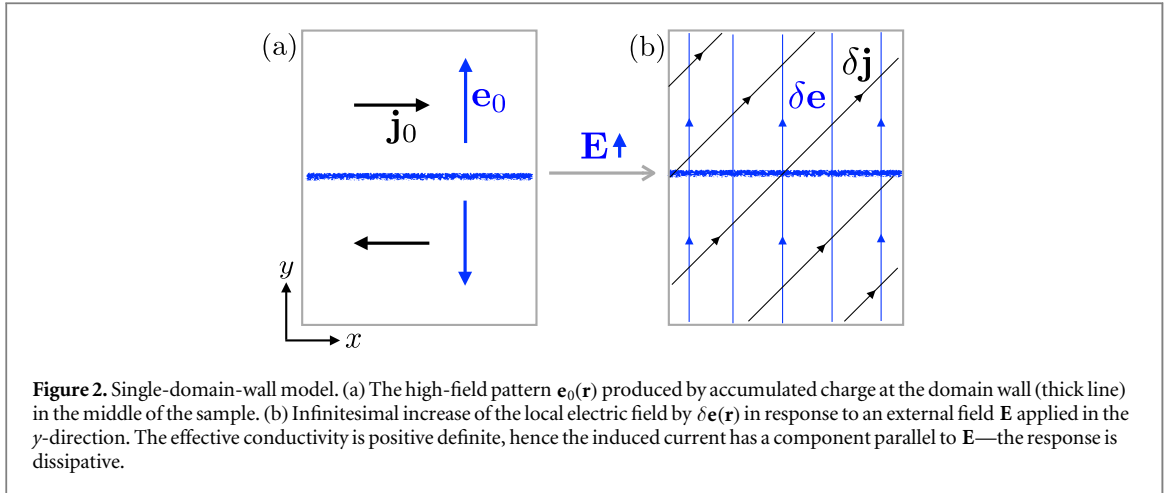


Figure 2. Single-domain-wall model. (a) The high-field pattern $\mathbf{e}_0(\mathbf{r})$ produced by accumulated charge at the domain wall (thick line) in the middle of the sample. (b) Infinitesimal increase of the local electric field by $\delta \mathbf{e}(\mathbf{r})$ in response to an external field \mathbf{E} applied in the y -direction. The effective conductivity is positive definite, hence the induced current has a component parallel to \mathbf{E} —the response is dissipative.

The dynamics are governed by the continuity equation, the Poisson equation, and Ohm's law,

$$\frac{d n(\mathbf{r}, t)}{dt} = -\nabla \cdot \mathbf{j}(\mathbf{r}, t), \quad (21a)$$

$$\mathbf{e}(\mathbf{r}, t) = -\nabla U n(\mathbf{r}, t) + \mathbf{E}, \quad (21b)$$

$$\mathbf{j}(\mathbf{r}, t) = \sigma(\mathbf{e}(\mathbf{r}, t)) \mathbf{e}(\mathbf{r}, t), \quad (21c)$$

where $U n(\mathbf{r}, t)$ is the electrostatic potential of the charge distribution, written in terms of a positive definite operator U , which encodes the Coulomb interaction, acting on the charge distribution. Considering U as a finite matrix with indices \mathbf{r} and \mathbf{r}' , its positive definiteness is due to the fact that the diagonal elements are infinite while the sum over each column or row is finite.

We decompose the charge density into $n(\mathbf{r}, t) = n_0(\mathbf{r}) + \delta n(\mathbf{r}, t)$, where $n_0(\mathbf{r})$ is the given charge density of the accumulated charge at the domain walls that produce the pattern $\mathbf{e}_0(\mathbf{r}) = -\nabla U n_0(\mathbf{r})$ and $\delta n(\mathbf{r}, t)$ is the time-dependent deviation induced by the external field. Then, as previously, the local electric field decomposes into the high-field pattern $\mathbf{e}_0(\mathbf{r})$ and the low-field pattern $\delta \mathbf{e}(\mathbf{r}, t) = -\nabla U \delta n(\mathbf{r}, t) + \mathbf{E}$ and the current density, to linear order in $\delta \mathbf{e}$, decomposes into $\mathbf{j}_0(\mathbf{r}) = \sigma(e_0) \mathbf{e}_0(\mathbf{r})$ and $\delta \mathbf{j}(\mathbf{r}, t) = \tilde{\sigma}(\mathbf{r}) \delta \mathbf{e}(\mathbf{r}, t)$, where $\tilde{\sigma}(\mathbf{r})$ is given in (9). The linearization of $\delta \mathbf{j}(\mathbf{r}, t)$ is valid as long as $|\delta \mathbf{e}(\mathbf{r}, t)| \ll e_0$.

Inserting into equation (21), we find the response entirely in the low-field subsystem, governed by

$$\frac{d \delta n(\mathbf{r}, t)}{dt} = -\nabla \cdot \delta \mathbf{j}(\mathbf{r}, t), \quad (22a)$$

$$\delta \mathbf{e}(\mathbf{r}, t) = -\nabla U \delta n(\mathbf{r}, t) + \mathbf{E}, \quad (22b)$$

$$\delta \mathbf{j}(\mathbf{r}, t) = \tilde{\sigma}(\mathbf{r}) \delta \mathbf{e}(\mathbf{r}, t). \quad (22c)$$

It is useful to consider ∇ , U , and $\tilde{\sigma}_{ij}(\mathbf{r})$ as matrices and $\delta e_i(\mathbf{r}, t)$, $\delta n(\mathbf{r}, t)$, E_i , and $\delta j_i(\mathbf{r}, t)$ as vectors by considering the spatial arguments as indices. Doing so and combining equations (22), we can write

$$\frac{d \delta n(t)}{dt} = -P \delta n(t) - \nabla_i \tilde{\sigma}_{ij} E_j, \quad P = \nabla_i^T \tilde{\sigma}_{ij} \nabla_j U, \quad (23)$$

where the sum over repeated indices $i, j \in \{x, y\}$ is implied and we used that ∇_i is skew symmetric. To bring equation (23) in the usual form of linear differential equations, we subtract the time-independent part, $\delta \bar{n}(t) = \delta n(t) - \delta n_0(E)$ with

$$P \delta n_0(E) = \nabla_i \tilde{\sigma}_{ij} E_j. \quad (24)$$

The solution $\delta \bar{n}(t) = 0$ of

$$\frac{d \delta \bar{n}(t)}{dt} = -P \delta \bar{n}(t) \quad (25)$$

is Lyapunov stable if the real parts of the eigenvalues of P are non-negative and those that are zero are semi-simple (i.e. its algebraic and geometric multiplicities coincide). That this is indeed the case can be seen by using the Cholesky decomposition $U = LL^T$ to obtain

$$P = (L^T)^{-1} M L^T, \quad M = L^T \nabla_i^T \tilde{\sigma}_{ij} \nabla_j L. \quad (26)$$

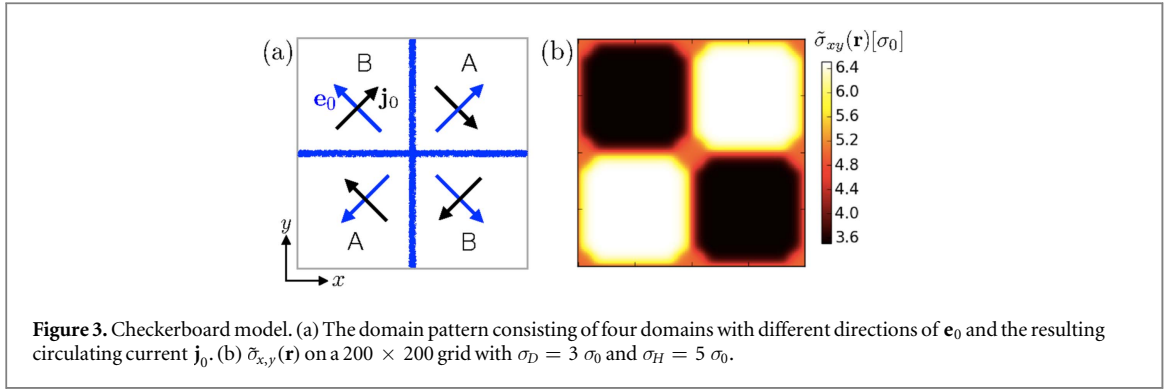


Figure 3. Checkerboard model. (a) The domain pattern consisting of four domains with different directions of \mathbf{e}_0 and the resulting circulating current \mathbf{j}_0 . (b) $\tilde{\sigma}_{x,y}(\mathbf{r})$ on a 200×200 grid with $\sigma_D = 3 \sigma_0$ and $\sigma_H = 5 \sigma_0$.

The symmetric part of M can be written as

$$M_S = \frac{M + M^T}{2} = L^T \nabla_i^T \frac{\tilde{\sigma}_{ij} + \tilde{\sigma}_{ji}}{2} \nabla_j L \quad (27)$$

$$= L^T \nabla_i^T \tilde{\sigma}_{S,ij} \nabla_j L, \quad (28)$$

where $\tilde{\sigma}_S$ is the symmetric part of $\tilde{\sigma}$. Similarly, the skew symmetric part M_A is given by the skew symmetric part of $\tilde{\sigma}$, which has $\pm\sigma_H$ on its off-diagonal. Since σ_H is \mathbf{r} independent, it commutes with ∇_i and we obtain

$$M_A = \sigma_H L^T [\nabla_y, \nabla_x] L = 0. \quad (29)$$

For an arbitrary vector ν we can thus write a square form as

$$\nu^T M \nu = V^T \tilde{\sigma}_S V, \quad (30)$$

where $V = (\nabla_x L \nu, \nabla_y L \nu)$ is a vector from a squared vector space compared to the vector space of ν . Since $\tilde{\sigma}_S$ is positive semidefinite in this squared vector space, we conclude that $\nu^T M \nu \geq 0$ for all ν , hence M is also positive semidefinite. Since $M_A = 0$, M is symmetric, consequently its eigenvectors are linearly independent. These properties are inherited by P because it is similar to M and we can conclude that the eigenvalues of P are non-negative and those which are zero belong to linearly-independent eigenvectors, are thus semi-simple. These are sufficient criteria for the Lyapunov stability of the steady solution $\delta \tilde{n}(t) = 0$, or equivalently $\delta n(t) = \delta n_0(E)$.

For $\mathbf{E} = 0$, the considerations above are essentially a revision of the arguments made in [12] on the stability of the state $\mathbf{e}(\mathbf{r}) = \mathbf{e}_0(\mathbf{r})$. For $\mathbf{E} \neq 0$, however, this shows that the linear-response states are also stable, although they deviate from $\mathbf{e}(\mathbf{r}) = \mathbf{e}_0(\mathbf{r})$ by $\delta \mathbf{e}(\mathbf{r})$ with $|\delta \mathbf{e}(\mathbf{r})| \ll e_0$.

A solution with the boundary condition $\delta n(t = 0) = 0$ reads

$$\delta n(t) = (1 - e^{-Pt}) \delta n_0(E), \quad (31)$$

from which we see that only the decaying non-zero modes of P contribute, which according to (24) scale with E .

Our main conclusion from this is that the application of an external field $E \ll e_0$ on a domain state with $\mathbf{e}(\mathbf{r}) = \mathbf{e}_0(\mathbf{r})$ will lead to small changes of the local electric field, which scale with E . In particular, this implies that the domain walls will not shift, since this would require $|\delta \mathbf{e}_0(\mathbf{r})| \sim e_0$.

We now demonstrate this behavior with two examples: the single-domain-wall model from the previous section and a C_4 symmetric model.

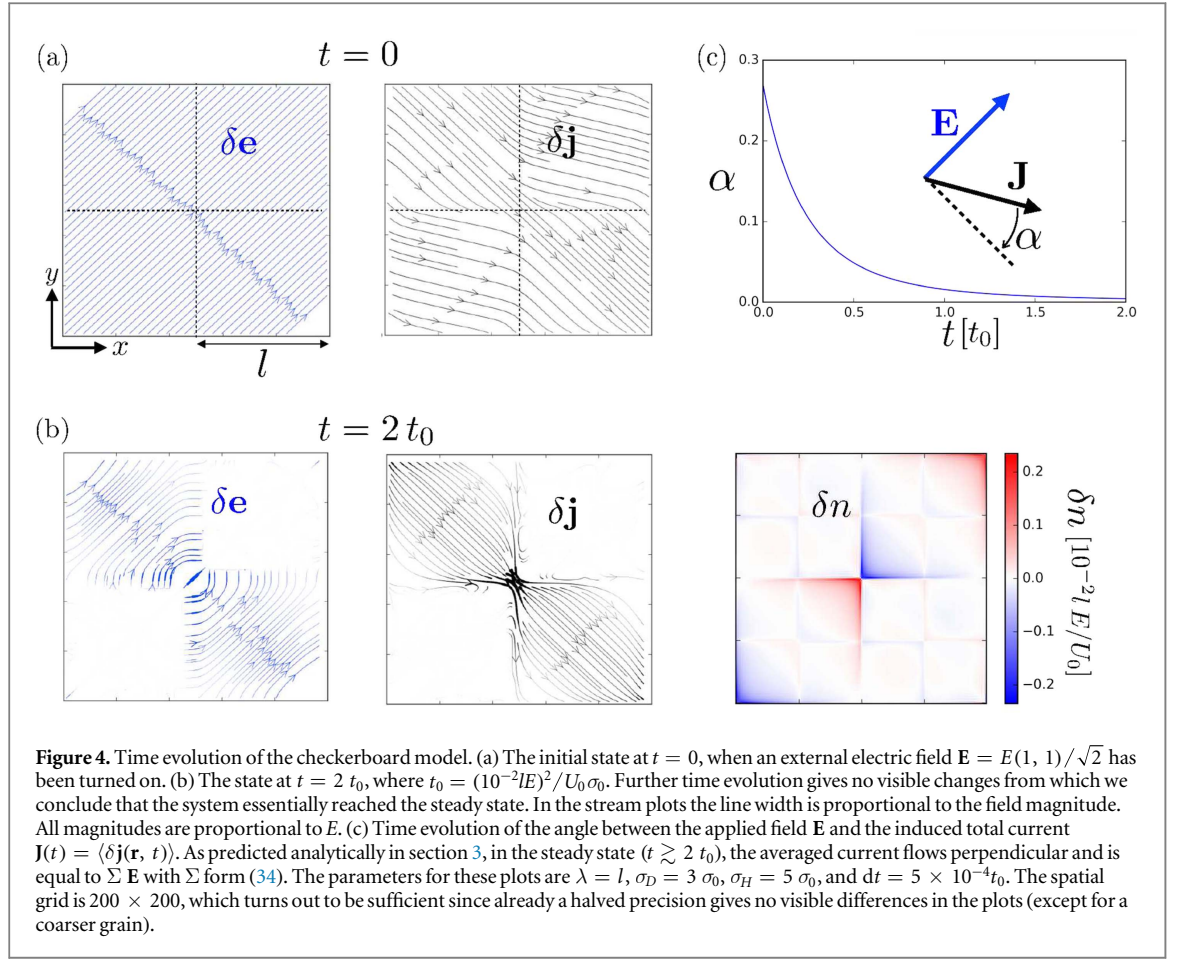
4.1. Single-domain-wall model

We consider again the single-domain-wall model shown in figure 2. Suppose that for $t < 0$ the domain state has the high-field pattern $\mathbf{e}_0(\mathbf{r})$ as shown in figure 2(a). At $t = 0$ we switch on an external electric field \mathbf{E} , so that $\delta \mathbf{e}(\mathbf{r}, t = 0) = \mathbf{E}$, as illustrated in figure 2(b). Since the local conductivity (19) is equal in both domains, the induced current density $\delta \mathbf{j}(\mathbf{r}, t = 0) = \tilde{\sigma}(\mathbf{r}) \mathbf{E}$ is \mathbf{r} -independent, hence $\nabla \cdot \delta \mathbf{j}(\mathbf{r}, t = 0) = 0$. From this follows immediately $\delta n(\mathbf{r}, t) = 0$, thus the system will remain in the $t = 0$ state, which is a linear-response state with $|\delta \mathbf{e}| = |\mathbf{E}| \ll e_0$.

For this particular domain pattern, the linear-response state coincides with the state at the instance when the electric field was switched on. In general, this is not true as is shown in the next example.

4.2. Checkerboard model

The domain pattern for this model is shown in figure 3(a). According to equation (9), the local conductivity in the domains A and B reads



$$\tilde{\sigma}(\mathbf{r}) = \begin{cases} \begin{pmatrix} \frac{\sigma_D}{2} & \sigma_H + \frac{\sigma_D}{2} \\ -\sigma_H + \frac{\sigma_D}{2} & \frac{\sigma_D}{2} \end{pmatrix} & \mathbf{r} \in A \\ \begin{pmatrix} \frac{\sigma_D}{2} & \sigma_H - \frac{\sigma_D}{2} \\ -\sigma_H - \frac{\sigma_D}{2} & \frac{\sigma_D}{2} \end{pmatrix} & \mathbf{r} \in B. \end{cases} \quad (32)$$

At $t = 0$, the local current density has a finite divergence, so the charge density will evolve, governed by equation (23). We simulate the time evolution numerically by discretizing the time with a finite time step dt and discretizing the space by an $N \times N$ grid with periodic boundary conditions in both directions. We measure the length in units of the domain length l , so that $\mathbf{r} = (x, y)$ with $x, y = 2li/N$, $i \in [0, N - 1]$.

To provide a reasonable description on the discretized space, we have to smoothen the domain boundaries over a few space points, i.e., find a continuous version of equation (32). To do so, we convolute the $N \times N$ matrices $e_{0,x}(\mathbf{r})$ and $e_{0,y}(\mathbf{r})$ with a Gaussian kernel of size $0.15 l$ and standard deviation $0.1 l$ to determine the continuous version of the angle $\phi(\mathbf{r}) = \arctan(e_{0,y}(\mathbf{r})/e_{0,x}(\mathbf{r}))$ in (9). At points where the angle is not defined, we suppress σ_D by the function $1/2 + \tanh[(|\mathbf{r}| - 0.15 l)/0.05 l]/2$. The resulting spatial dependence of $\tilde{\sigma}$ is shown in figure 3(b). We checked that the variation of these parameters does not have qualitative influence on the result.

We approximate the action of the interaction operator U on δn by a convolution of δn with a kernel

$$U_{x,y} = \frac{U_0}{\sqrt{(x^2 + y^2)/\xi^2 + \eta^2}} \quad (33)$$

of size $\lambda \times \lambda$ and with parameters set to $\xi = 0.1 l$ and $\eta = 10^{-2}$ (η can be seen as a finite out-of-plane component and we consider numerically the limit $\eta \rightarrow 0$). The variation of these parameters and the size of the kernel within the physical parameter regime (which is restricted by the requirement of a positive definiteness of U), does not lead to qualitative differences. Representative numerical results are summarized in figure 4.

As predicted by our symmetry considerations, in the steady state the average current flows perpendicular to the applied field, according to the simple relation $\mathbf{J} = \Sigma \mathbf{E}$ with

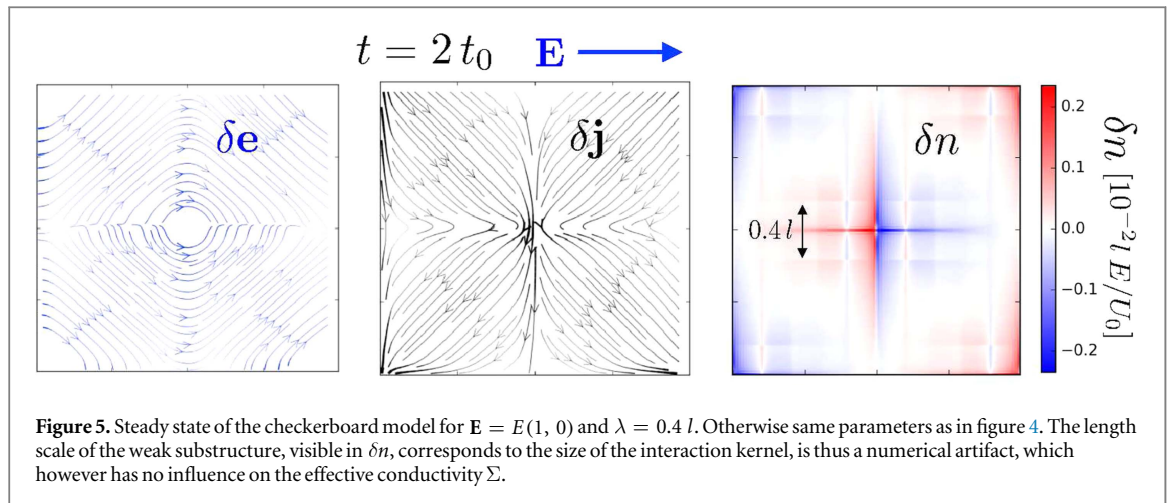


Figure 5. Steady state of the checkerboard model for $\mathbf{E} = E(1, 0)$ and $\lambda = 0.4 l$. Otherwise same parameters as in figure 4. The length scale of the weak substructure, visible in δn , corresponds to the size of the interaction kernel, is thus a numerical artifact, which however has no influence on the effective conductivity Σ .

$$\Sigma = \begin{pmatrix} 0 & \sigma_H \\ -\sigma_H & 0 \end{pmatrix}. \quad (34)$$

In contrast to this, the local fields and the charge density acquire a non-universal structure during the evolution, which depends on the details of the interaction, domain length, and the direction of the applied electric field. This dependence is illustrated in figure 5, where we show plots of the steady state for the electric space field $\mathbf{E} = E(1, 0)$ and $\lambda = 0.4 l$ (compare with figure 4: $\mathbf{E} = E(1, 1)/\sqrt{2}$ and $\lambda = 1 l$). Comparing the figures, we see that the local field patterns change dramatically. The effective conductivity (34) stays the same.

It is interesting to compare this ZRS to the quantum Hall effect for magnetic fields at the Hall plateaus. The Hall effect also shows a purely transversal resistance, hence a very similar macroscopic response. The microscopic current flow, however, turns out to be different: while in the Hall effect bulk states are localized and current is carried entirely by the edge states, in the domain state current flows through the bulk, albeit in an inhomogeneous pattern.

5. Conclusion

In conclusion, we have considered the response of domain states to external fields (induced by a dc voltage) that are much smaller than the internal fields within the domains (induced by microwave radiation). We have proposed a new response mechanism, which, contrary to the established one, does not involve domain-wall shifting. In our view, small external fields lead only to small modulations of the local fields, leaving the domain patterns unchanged. The theoretical justification of the linear scenario is based on the fact that small deviations from the pure domain state are not unstable, which we have shown by analyzing the electrodynamics of a general domain state. We tested these predictions on two specific realizations numerically.

Our main results address the effective conductivity of the domain state in the linear scenario: if the effective conductivity is isotropic, which is the case if the domain pattern is chaotic or C_4 symmetric, then the response is dissipationless. Otherwise the response can be dissipative, which we have shown for the single-domain-wall pattern—the energetically most favorable pattern in a clean system [12].

Combining this result with the fact that disorder can pin the domain walls in a chaotic pattern [13, 14], this work supports the idea that the radiation-induced ZRS is a disordered domain state, where the disorder is strong enough to allow for a chaotic domain pattern. Clean domain states, instead, are allowed to have a dissipative response. The explicit value of the longitudinal conductivity is presumably non-universal in this case. This is in stark contrast to the domain-wall response, which predicts strictly zero-resistance in the clean case and dissipative response in the regime of pinned domain walls [13].

Measurements that are sensitive to local changes of the electric field [20, 21] indicate that the domain structure is indeed rather complex and show that the local electric fields change proportional to the applied voltages. These observations, hard to reconcile with the domain-wall-response scenario, are in qualitative agreement with our theory.

We stress that this work is based on the assumption that the system is in a domain state, which at present appears to be the dominant picture for the ZRS but not indisputably established one. Steadiness of the domain pattern is also an essential ingredient for our analysis, which is a justified assumption in radiation-induced ZRS [15, 19]. Time-dependent patterns, however, may occur in many other cases, e.g., including the zero-differential-resistance states in dc biased 2D electron gases in strong magnetic fields [24], where the domain

structure moves between boundaries of the sample. The extension of the present analysis to time-dependent domain patterns remains a subject for future work.

Acknowledgments

Discussions with C Timm and F von Oppen are gratefully acknowledged. This work is financed by the Netherlands Organisation for Scientific Research (NWO).

References

- [1] Mani R G, Smet J H, von Klitzing K, Narayanamurti V, Johnson W B and Umansky V 2002 *Nature* **420** 646
- [2] Zudov M A, Du R R, Pfeiffer L N and West K W 2003 *Phys. Rev. Lett.* **90** 046807
- [3] Dmitriev I A, Mirlin A D, Polyakov D G and Zudov M A 2012 *Rev. Mod. Phys.* **84** 1709
- [4] Mikhailov S A 2011 *Phys. Rev. B* **83** 155303
- [5] Chepelianskii A D and Shepelyansky D L 2009 *Phys. Rev. B* **80** 241308
- [6] Herrmann T *et al* 2016 *Phys. Rev. B* **94** 081301
- [7] Iñarrea J and Platero G 2005 *Phys. Rev. Lett.* **94** 016806
- [8] Durst A C, Sachdev S, Read N and Girvin S M 2003 *Phys. Rev. Lett.* **91** 086803
- [9] Vavilov M G and Aleiner I L 2004 *Phys. Rev. B* **69** 035303
- [10] Dmitriev I A, Vavilov M G, Aleiner I L, Mirlin A D and Polyakov D G 2005 *Phys. Rev. B* **71** 115316
- [11] Beltukov Y M and Dyakonov M I 2016 *Phys. Rev. Lett.* **116** 176801
- [12] Andreev A V, Aleiner I L and Millis A J 2003 *Phys. Rev. Lett.* **91** 056803
- [13] Auerbach A, Finkler I, Halperin B I and Yacoby A 2005 *Phys. Rev. Lett.* **94** 196801
- [14] Finkler I, Halperin B I, Auerbach A and Yacoby A 2006 *J. Stat. Phys.* **125** 1093
- [15] Finkler I G and Halperin B I 2009 *Phys. Rev. B* **79** 085315
- [16] Dmitriev I A, Khodas M, Mirlin A D and Polyakov D G 2013 *Phys. Rev. Lett.* **111** 206801
- [17] Mani R G and Kriisa A 2013 *Sci. Rep.* **3** 3478
- [18] Zakharov A L 1960 *JETP* **11** 478
- [19] Dorozhkin S I, Pfeiffer L, West K, von Klitzing K and Smet J H 2011 *Nat. Phys.* **7** 336
- [20] Dorozhkin S I, Umansky V, Pfeiffer L N, West K W, Baldwin K, von Klitzing K and Smet J H 2015 *Phys. Rev. Lett.* **114** 176808
- [21] Dorozhkin S I, Umansky V, Von Klitzing K and Smet J H 2016 *JETP Lett.* **104** 721
- [22] Dykhne A M and Kaganova I M 1997 *Phys. Rep.* **288** 263
- [23] Dykhne A M 1971 *JETP* **32** 63
Dykhne A M 1971 *JETP* **32** 348
- [24] Bykov A A, Zhang J-Q, Vitkalov S, Kalagin A K and Bakarov A K 2007 *Phys. Rev. Lett.* **99** 116801